Magnetic Properties of Nanometer-Scale Iron Particles Generated by Iron Atom Clustering in Cold Pentane

Carl F. Kernizan,[1] Kenneth J. Klabunde,*[,1] Christopher M. Sorensen,[2] and George C. Hadjipanayis[2]

Departments of Chemistry and Physics, Kansas State University, Manhattan, Kansas 66506

Received July 20, 1989

Nanometer-scale iron particles have been prepared by iron atom clustering in cold pentane. Particle growth was terminated by adsorption of oleic acid, yielding air-stable particles ranging in size from 2 to 12 nm, that were amorphous according to XRD analysis. TEM analysis showed that the larger particles were prolate spheroids and the smaller ones were spherical. The original sample had a room-temperature saturation magnetization of M_s = 12.3 emu/g and a coercivity of H_c = 60 Oe. Following heat treatment with argon, the XRD results showed the following reaction scheme: oxidation to Fe_3O_4 at 360 °C and reduction to α-Fe at 520 °C (processes apparently due to adsorbed oleic acid). For the 520 °C treated sample, the room-temperature saturation magnetization and coercivity were M_s = 200 emu/g and H_c = 20 Oe, respectively. By pentane washing of the as-prepared sample, the smaller particles could be separated by filtration, leaving the larger 8–12-nm particles on the filter. This powdered sample trapped on the filter had M_s = 54.9 emu/g and H_c = 60 Oe. Heat treatment also caused oxidation to Fe_3O_4 at 360 °C and an incomplete reduction to α-Fe and FeO at 520 °C. For the 520 °C treated sample, the recorded room-temperature saturation magnetization and coercivity were M_s = 123.6 emu/g and H_c = 20 Oe, respectively.

Introduction

The preparation and properties of very small particles often called "clusters" or "nano-scale materials" have been of great interest in recent years.[3] Particles of 1–100 nm often exhibit hybrid properties different from those molecular or atomic species and different from the bulk solid state.

One approach in making metallic clusters is by atom agglomeration in inert gases or in low-temperature liquids. In fact both media have yielded metal clusters possessing unusual reactivities,[4,5] and we believe kinetic control of growth in cold liquids leads to metastable states that possess many reactive surface sites.[5]

A challenge in this field of nanometer-scale materials is to make large amounts (grams) of single-phase materials protected from oxidation. Our approach has been to deposit metal atoms into low-temperature organic solvents, which leads to atom clustering moderated by solvation (solvated metal atom dispersion (SMAD)).[6] Trapping the small clusters on high-surface-area supports has led to the synthesis of a wide series of unique monometallic and bimetallic heterogeneous catalysts.[7] The small clusters are protected somewhat by solvation toward further particle growth, although protection from oxidation by the atmosphere is not adequate without additional procedures.

For magnetic materials prepared by similar methods three factors have been found to affect their magnetization: surface oxide formation, inhomogeneous particle size distribution, and carbonaceous fragment inclusion within these particles.[8-10] The nature of these problems implies that they might be solved by varying the metal–solvent interaction. Recently, Timms and co-workers,[9] using metal atom deposition/clustering in liquids, have reported that they were successful in controlling some of these problems by adding a surfactant to the host solvent during metal evaporation. This modification in their method closely follows the preparation of ferrofluids. Ferrofluids are suspended magnetic particles in a carrier solvent with an added surfactant to make the suspension stable.[11-15] The surfactants of choice are long-chained hydrocarbons with carboxylic end groups or polymers with multiple carboxylic end groups.[12] Presumably the addition of a surfactant serves a 3-fold purpose. The first is that the polar end group adsorbs to the surface of the particle and prevents further oxidation, second the long-chained hydrocarbon end prevents agglomeration by sterically hindering dipolar attractions, and third the surfactant enhances "solubility" in the organic fluid.

Several other research teams have synthesized nanometer-scale metallic particles in polymer oils by similar techniques.[16,17] However, what has been lacking in all this work is the isolation, purification, and characterization of such metallic particles.

In this paper we wish to report that we have successfully

---

(1) Department of Chemistry.

(2) Department of Physics.

(3) Andres, R. P.; Averback, R. S.; Brown, W. L.; Brus, L. E.; Goddard, W. A.; Kaldor, A.; Louie, S. G.; Moscovits, M.; Peercy, P. S.; Riley, S. J.; Siegel, R. W.; Spaepen, F.; Wang, Y. *J. Mater. Res.* **1989**, *4*, 704–736.

(4) Kaldor, A.; Cox, D. M.; Zakin, M. R. In Molecular Surface Chemistry: Reactions of Gas Phase Metal Clusters. *Adv. Chem. Phys.* **1988**, *70*, 211.

(5) Klabunde, K. J.; Jeong, G. H.; Olsen, A. W. *Molecular Structure and Energetics*; Liebman, J. F., Greenberg, A., Eds.; VCH Publishers: New York; C-H Activation Chapter, in press.

(6) Klabunde, K. J.; Tanaka, Y. *J. Mol. Catal.* **1983**, *21*, 57.

(7) Klabunde, K. J.; Davis, S. C.; Hattori, H.; Tanaka, Y. *J. Catal.* **1978**, *54*, 254. Klabunde, K. J.; Ralston, D.; Zoellner, R.; Hattori, H.; Tanaka, Y. *J. Catal.* **1978**, *55*, 213. Davis, S. C.; Klabunde, K. J. *J. Am. Chem. Soc.* **1978**, *100*, 5973.

(8) Scott, B. A.; Plecenik, R. M.; Cargill, G. S., III; McGuire, R. T.; Head, S. *Inorg. Chem.* **1980**, *19*, 1252.

(9) Kilner, M.; Mason, N.; Lambrick, D. B.; Hooker, P. D.; Timms, P. L. *J. Chem. Soc., Chem. Commun.* **1987**, 357.

(10) Nakatani, I.; Furubayashi, T.; Takahashi, T.; Hanaoka, H. *J. Magn. Magn. Mater.* **1987**, *65*, 261.

(11) Rosenweig, R. E. Ferrohydrodynamics: Fluids for Direct Conversion of Heat Energy. *ICHE Symp. Ser.* **1965**, *5*, 104.

(12) Berkovsky, B. *Thermodynamics of Magnetic Fluids: Theory and Applications*; Hemisphere Publishing Co., 1978.

(13) Scholten, P. C.; "Colloid Chemistry of Magnetic Fluids in Thermomechanics of Magnetic Fluids," ed., Berkovsky, B.; Hemisphere Pub. Co., 1978.

(14) Charles, S. W.; Popplewell, J.; "The Preparation and Properties of a Stable Metallic Ferrofluid, in Thermodynamics of Magnetic Fluids", ed. Berkovsky, B.; Hemisphere: New York, 1978.

(15) Popplewell, J. *Endeavor* **1982**, *6*, 153.

(16) Andrews, M. P.; Ozin, G. A. *Chem. Mater.* **1989**, *1*, 174.

(17) Furubayashi, T.; Nakatani, I. *Proc. Int. Symp. Phys. Magn. Mater. Sindai Japan* **1987**, 182.

0897-4756/90/2802-0070$02.50/0

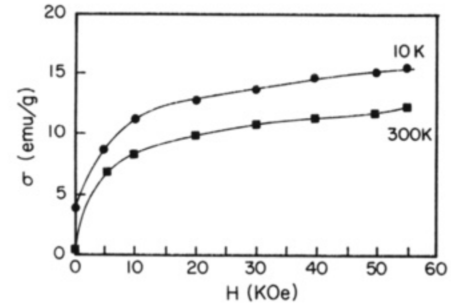

Figure 1. Magnetization as a function of the applied field for sample 1.

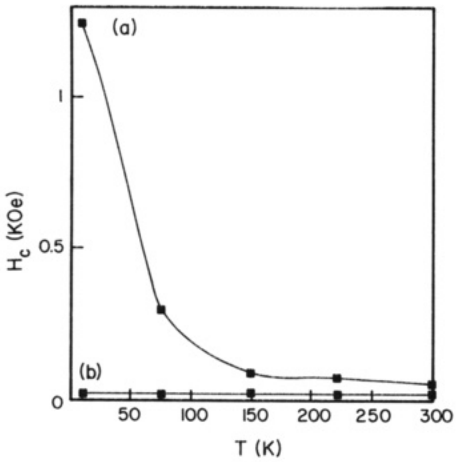

Figure 2. Coercivity as a function of temperature for sample 1: (a) untreated 1; (b) 3 heat treated at 520 °C.

Scheme I[a]

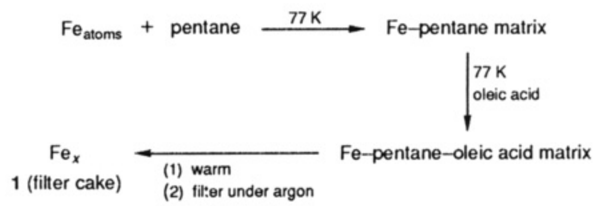

[a] Oleic acid signifies $HOC(O)(CH_2)_7CH{=}CH(CH_2)_7CH_3$ and/or fragments.

generated nanometer-scale iron clusters trapped and protected by adsorbed oleic acid. These particles are air stable and can be separated into superparamagnetic and ferromagnetic fractions by filtration/washing techniques. We have characterized their magnetic properties thoroughly and have monitored changes with heat treatment. We believe that the knowledge gained from this study might prove valuable in the preparation of other normally air-sensitive magnetic materials.

Experimental Section

Our metal atom (vapor) reactor has been described elsewhere.[18,19] A solvent inlet with two ports was used in this work so that initially iron atoms and pentane vapor could be co-deposited at 77 K. Later a pentane–oleic acid solution was added as a liquid (Fe:pentane:oleic acid 1:40:2 molar ratio). After the reaction chamber was allowed to slowly warm to room temperature, the sample was collected by vacuum syphoning onto a fritted filter under pure argon. Filtration and washing with more pentane yielded two fractions. The ferromagnetic fraction remained on

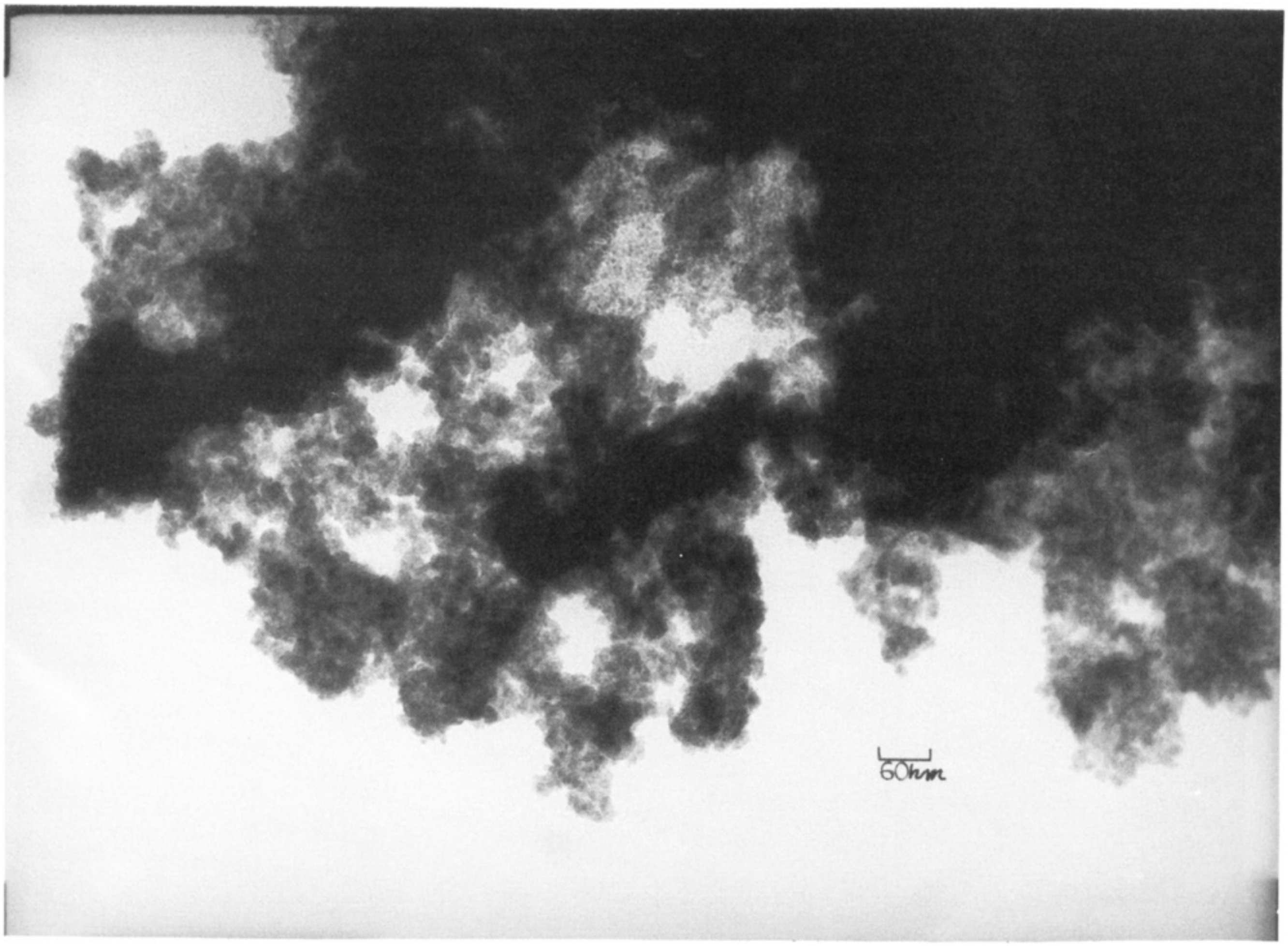

Figure 3. TEM micrograph of sample 1. Samples were prepared by placing sample 1 in acetone and treated by ultrasound for 5–10 min. The resultant colloidal solution was dripped onto carbon-coated copper grids, followed by solvent evaporation.

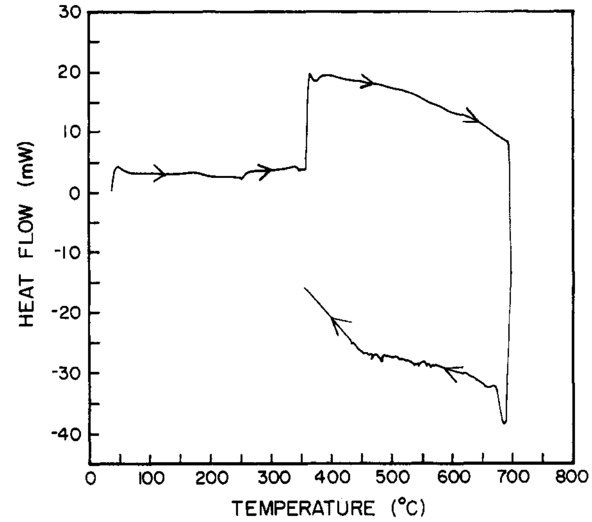

Figure 4. DSC measurement of sample 1.

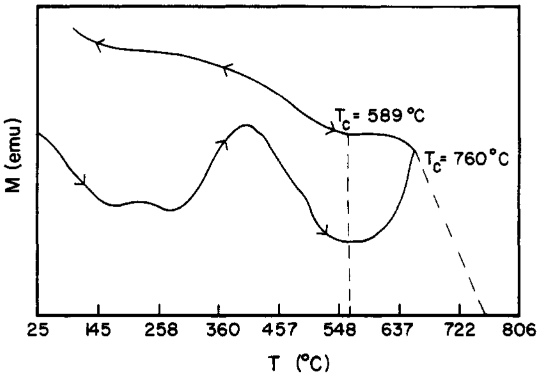

Figure 5. Temperature dependence of the magnetization and Curie point measurement for sample 1.

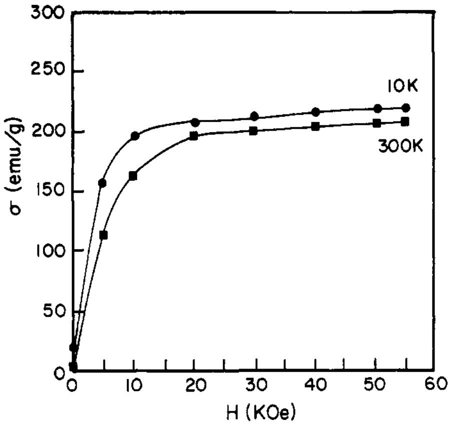

Figure 6. Magnetization as a function of the applied field for sample 3.

the frit as a black powder while the superparamagnetic fraction filtered through and formed a colloidal suspension (ferrofluid in pentane).

Heat treatments were carried out in an autoclave at 386 and 520 °C for 6 h under flowing argon.

A SQUID magnetometer was used to determine magnetic properties (weighed samples were embedded in paraffin), and a

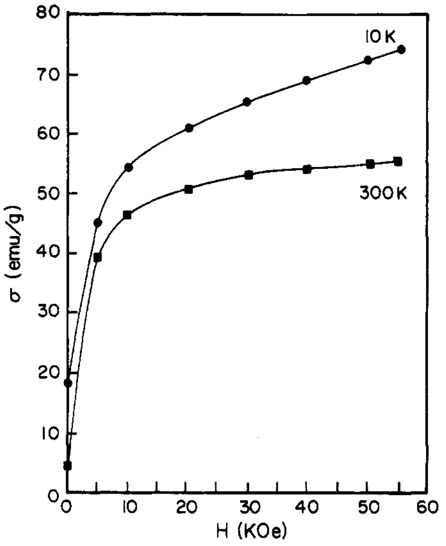

Figure 7. Magnetization as a function of the applied field for sample 4.

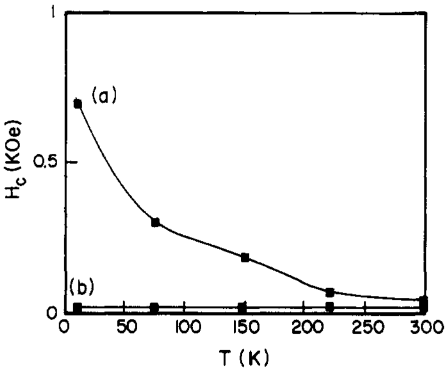

Figure 8. Coercivity as a function of temperature for sample 4; (a) untreated 4; (b) 4 heat treated at 520 °C.

high-temperature VSM to obtain Curie temperatures. Other techniques such as TEM, DSC, and XRD were also used to determine sizes and morphologies of these particles.

Results and Discussion

Iron atoms were condensed with a 40-fold excess of pentane to form a dark matrix at 77 K. Then a pentane–oleic acid solution was allowed to freeze on top of the matrix. Upon warming, the iron atoms agglomerated to clusters, which were trapped and stabilized by the oleic acid (Scheme I).

Figure 1 illustrates magnetization as a function of applied field for sample 1. The room-temperature magnetization at a field of 55 kOe was only 12.4 emu/g as compared to the bulk iron metal value of 220 emu/g.[20] This low value is not surprising since the sample consisted of a range of very small particles. Sample 1 was air stable, presumably due to protection by adsorbed oleic acid. The coercivity plotted as a function of temperature, Figure 2a, was high at 10 K, H_c = 1260 Oe, and decreased to 60 Oe at 300 K. These high values might be due to a phenomenon called "exchange anisotropy" which describes the spin coupling at the interface of these iron particles and the organic coating.[21-23]

XRD analysis of 1 showed that it was amorphous. The TEM micrograph measurements showed particles ranging

---

(18) Klabunde, K. J.; Timms, P. L.; Skell, P. S.; Ittel, S. *Inorg. Synth.* **1979**, *19*, 59.

(19) Groshens, T. J.; Klabunde, K. J. *Experimental Organometallic Chemistry*; Wayda, A. L.; Darensbourg, M. Y., Eds.; ACS Symposia Series, No. 357; American Chemical Society: Washington, DC, 1987; pp 190, 193.

(20) Cullity, B. D. *Introduction to Magnetic Materials*; Addison-Wiley: New York, 1972; pp 171–190.

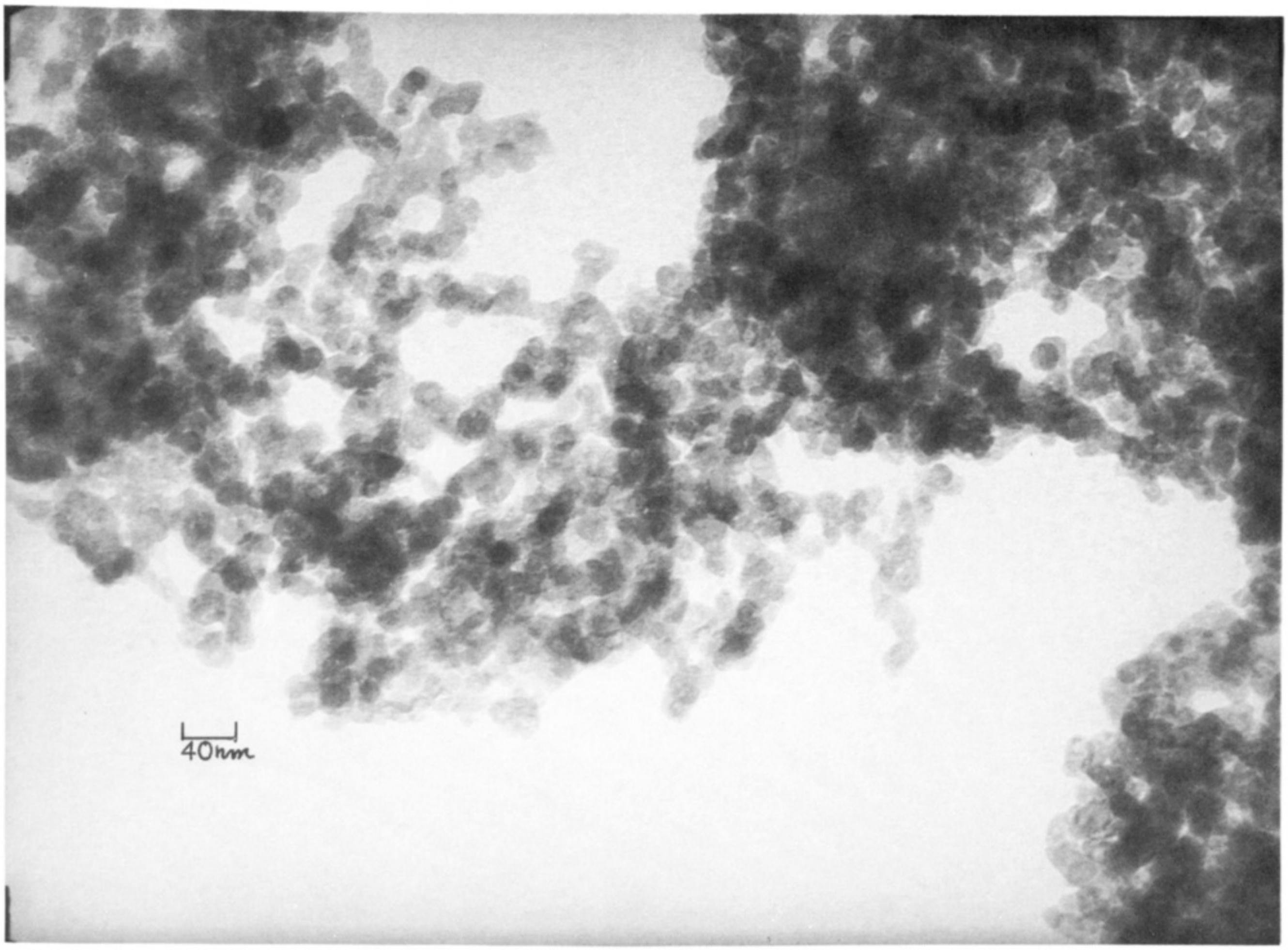

Figure 9. TEM micrographs of sample **4**. Samples were prepared by placing sample **4** in acetone and treated by ultrasound for 5–10 min. The resultant colloidal solution was dripped onto carbon-coated copper grids, followed by solvent evaporation.

in size from 2 to 12 nm in diameter that resembled distorted spheres (Figure 3). Analysis by DSC indicated a sharp exothermic peak at 360 °C and a gradual decrease to 700 °C (Figure 4). The temperature dependence of the magnetization and the Curie point measurements shown in Figure 5 were in good agreement with the previous DSC measurements. The curve at increasing magnetic field shows a phase change at 360 °C and an additional phase change around 600 °C. Two Curie points at 589 and 760 °C were measured by extrapolation for these two phases.

Following the M vs T and the DSC results, we heat treated **1** at 386 and 520 °C under flowing argon for 6 h. XRD results obtained after heat treatment at both temperatures showed that **1** followed the reaction scheme

$$\mathbf{1} \xrightarrow[\text{argon}]{386\ ^\circ\text{C}} \underset{\mathbf{2}}{\mathrm{Fe_3O_4}} \xrightarrow[\text{argon}]{520\ ^\circ\text{C}} \underset{\mathbf{3}}{\alpha\text{-Fe (metallic iron pellet)}}$$

At the lower temperature, **1** was oxidized to form Fe_3O_4 probably by the cleavage of the oxygen from the carboxylate end of the oleic acid. At higher temperatures, the resultant magnetite was reduced apparently by excess carbon, to α-Fe (iron pellet), with a 10% weight loss. Even though this reaction scheme is consistent with the data obtained, none of our testing methods could account for the presence of the excess carbon as carbides. Both Curie points at 589 and 760 °C were in good agreement with the reported values for Fe_3O_4 and α-Fe.[20]

The magnetization curve of **3** is shown in Figure 6; a very high room-temperature saturation magnetization value of 200 emu/g was recorded, which is about 90% of the value for bulk iron.[20] The coercivity plotted as a function of temperature (Figure 2b) gave values of 20 Oe at all temperatures. These results can be explained by small-particle sintering (**1** → **3**), and upon formation of **3**, the pellet experienced a significant decrease in the exchange anisotropy.

Sample **1** was fractionated by washing with pentane. In this way the larger particles (8–12 nm) remained on the frit while smaller ones (2–7 nm) were soluble and were obtained in the filtrate suspended in pentane:

$$\mathbf{1} \xrightarrow[\text{wash}]{\text{pentane}} \underset{\substack{\mathbf{4}\\ \text{ferromagnetic}\\ \text{(filter cake)}}}{\mathrm{Fe}_y} + \underset{\substack{\mathbf{5}\\ \text{superparamagnetic}\\ \text{(filtrate)}}}{\mathrm{Fe}_z}$$

$$y > z, \text{ the size of } \mathrm{Fe}_y \approx 8\text{–}12 \text{ nm}$$

$$\text{the size of } \mathrm{Fe}_z \approx 7\text{–}2 \text{ nm}$$

Sample **4** was also amorphous according to XRD.

The magnetization curve for **4** is shown in Figure 7; **4** had a room-temperature magnetization of 54.9 emu/g, or 23% higher than the value obtained for **1**. This result corroborated the fact that after being washed with excess pentane, the smaller particles were absent from **4**. The

---

(21) Berkowitz, A. E. *IEEE Trans. Magn.* **1986**, *MAG-22*, *5*, 466.
(22) Meiklejohn, W. H.; Bean, C. P. *Phys. Rev.* **1956**, *102*, 1413; **1957**, *105*, 904.
(23) Meiklejohn, W. H. *J. Appl. Phys.* **1962**, *33*, 1328.

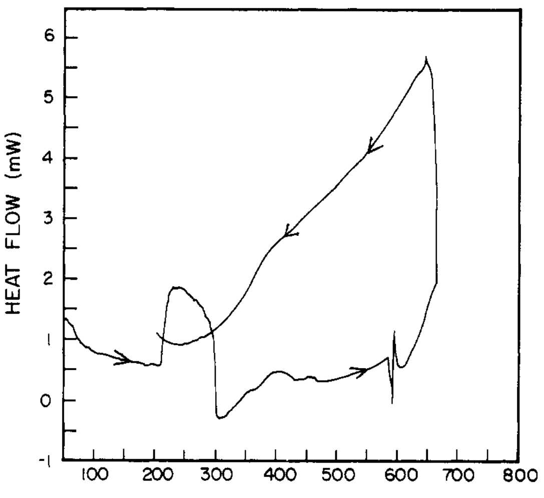

Figure 10. DSC measurements of sample 4.

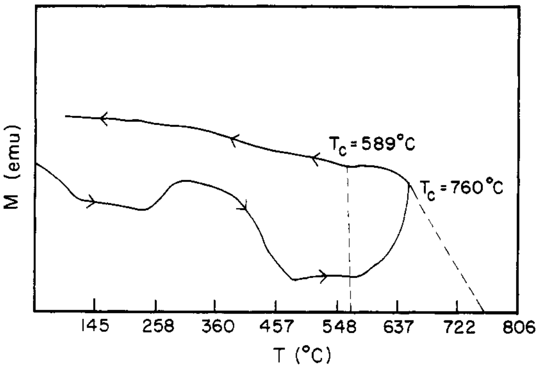

Figure 11. Temperature dependence of the magnetization and Curie point measurement for sample 4.

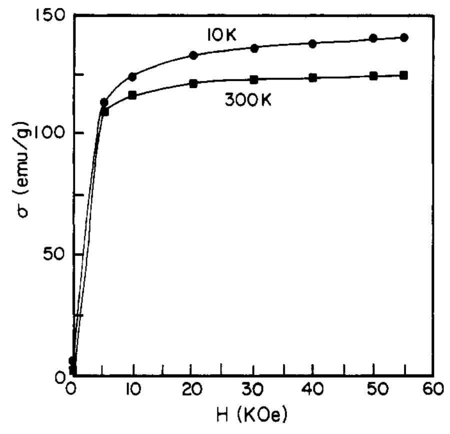

Figure 12. Magnetization as a function of applied field for sample 6.

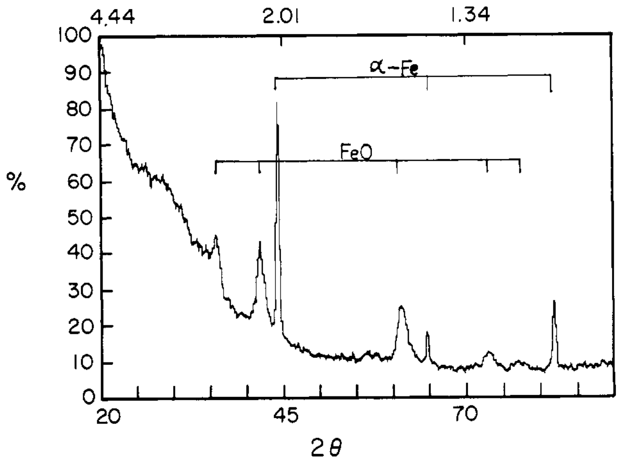

Figure 13. XRD analysis of sample 6.

magnetic properties and physical appearance of **4** did not change over a 3-month exposure to air at room temperature. This remarkable air stability for a fine powder indicates that the oleic acid is very effective at protecting the particle surfaces. Figure 8a shows the coercivity plotted as a function of the temperature. At 10 K the value dropped to 700 Oe but leveled to 60 Oe at 300 K, similar to sample 1. From the TEM micrograph (Figure 9), we observed particles that were prolate spheroids (oblong, peanut shapes) with average dimensions of 12 × 8 nm. A DSC study, Figure 10, did not show a sharp peak around 360 °C as was observed in **1**. Instead, two exothermic peaks between 220–300 and 600 °C were observed. The first phase transition was again due to the formation of Fe_3O_4 and the second to the formation of α-Fe. A VSM study of the process confirmed this behavior (compare Figures 5 and 11). Again both measured Curie temperatures were in very good agreement with the reported values of Fe_3O_4 and α-Fe.

Heat treatment of **4** at 520 °C under flowing argon produced a powder containing many metallic whiskers, **6**. Figure 12 shows the magnetization curve of **6**; a sharp increase in the saturation magnetization was observed with M_s = 138.7 (10 K) and 123.6 emu/g (300 K). Similar to the conversion **1** → **3**, the conversion of **4** → **6** caused the coercivities to decrease to ~20 Oe; see Figure 8b. The XRD analysis (Figure 13) showed that **6** consisted of mainly α-Fe with some FeO.

These results show that sample **4**, consisting of prolate spheroids stabilized by oleic acid, possessed soft magnetic character. Upon heating, oxidation to Fe_3O_4 occurred over the 220–400 °C range. Finally, at higher temperatures, reduction followed to form the second phase at 600 °C. But due to the decreased amount of carbon present following the pentane washing, complete reduction could not be achieved. Instead XRD shows the presence of both FeO and α-Fe in contrast to the scheme followed by **1** → **3**. Finally, the presence of FeO explains the lowered saturation magnetization value of 123.6 emu/g recorded for **6** as compared to the value of 200 emu/g obtained for **3**.

Conclusions

Nanometer-scale iron particles have been prepared by iron atom clustering in cold pentane. These particles have been stabilized toward further growth and oxidation by coordinating oleic acid. The smaller particles so stabilized are somewhat soluble in pentane and can be separated by filtration and pentane washing. The larger particles showed high coercivities at low temperature due to the presence of exchange anisotropy. Analysis by TEM showed that the total particle sizes ranged from 2 to 12 nm and the larger ones were prolate shaped. Heat treatment under flowing argon suggest that an oxidation at 386 °C to Fe_3O_4 occurred and reduction at higher temperatures to α-Fe and FeO depended on the amount of organic carbon present. After heat treatment the magnetization values increased while the coercivities sharply decreased due to the absence of exchange anisotropy.

Acknowledgment. The support of the National Science Foundation Materials Chemistry Initiative (CHE-8706954) is acknowledged with gratitude.

Registry No. Fe_3O_4, 1317-61-9; FeO, 1345-25-1; iron, 7439-89-6; pentane, 109-66-0.